

RESEARCH ARTICLE | SEPTEMBER 14 2022

Study of the plasticity of magnesium alloy MA2-1 based on torsion tests of cylindrical specimens

Yu. V. Zamaraeva ; Y. N. Loginov; M. V. Erpalov

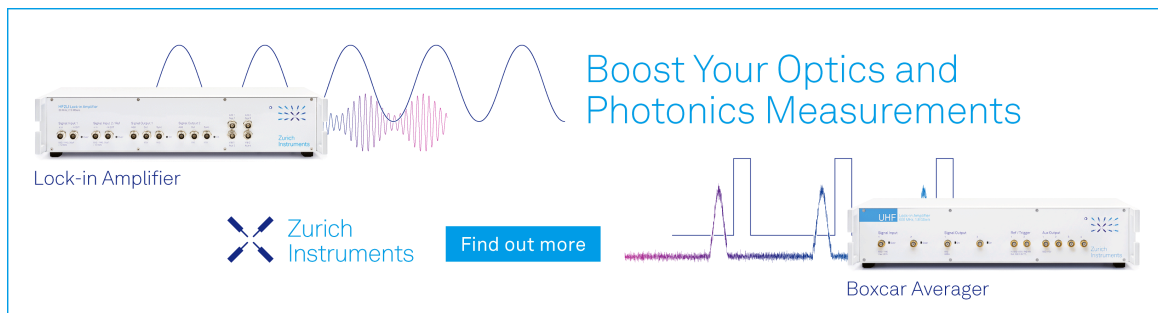


AIP Conf. Proc. 2533, 020042 (2022)


<https://doi.org/10.1063/5.0099027>



Boost Your Optics and Photonics Measurements



Lock-in Amplifier



[Find out more](#)

Boxcar Averager

Study of the Plasticity of Magnesium Alloy MA2-1 Based on Torsion Tests of Cylindrical Specimens

Yu. V. Zamaraeva^{1, 2, a)}, Y. N. Loginov^{1, 2}, M. V. Erpalov¹

¹*Ural Federal University, 19 Mira Str., Ekaterinburg, 620002, Russia*

²*M. N. Mikheev Institute of Metal Physics of Ural Branch of Russian Academy of Sciences, 18 S. Kovalevskaya Str., Ekaterinburg, 620108, Russia*

a) Corresponding author: zamaraevajulia@yandex.ru

Abstract. Magnesium and its alloys are of great interest for the study of their properties, in particular, necessary for the development of technologies for the manufacture of products in demand. This paper presents the results of studies of the plasticity of magnesium alloy MA2-1 based on the results of torsion tests of cylindrical specimens. A technique is proposed for measuring strain inhomogeneity along the specimens. Based on a comparison of the data on the distribution of shear strain and the loading diagram, the value of ultimate plasticity was established equal to $\Lambda_{ult} = 0.34 \dots 0.36$.

INTRODUCTION

Research in the field of the deformation of magnesium and its alloys is currently relevant due to the expansion of using these materials in various industries [1–3]. Magnesium, which has a hexagonal close-packed (HCP) crystal lattice, has a limited number of slip planes, which means the reduced plasticity at room temperature [4–6]. Therefore, magnesium and its alloys have to be deformed in a hot or warm state. However, there is a tendency to deform them at room temperature, because this makes it possible to preserve the strain hardening obtained during deformation [7, 8]. However, to develop methods for cold deformation of magnesium and its alloys, it is necessary to have information about the plasticity of the material. To study plasticity, various methods of deformation are used, for example, compression [9], tension [10], multiaxial loading methods [11], etc.

This paper presents the results of testing specimens of the MA2-1 alloy following the Russian standard GOST 14957. This alloy is an approximate analog of the ASTM B90 AZ31 alloy. Therefore, some known information about testing the AZ31 alloy is presented below.

The authors of [12] analyzed the failure of a sheet specimen made of AZ31 magnesium alloy at elevated temperatures. For this, they developed a heating unit for uniaxial tensile testing machines. In [13], several tests were carried out at room temperature under various loading conditions to obtain the characteristics of plasticity and fracture of cold-rolled sheet specimens made of AZ31B-H24 alloy. The authors of [14] considered the effect of twinning on the mechanical behavior of specimens from the extruded AZ31 alloy during torsion. In this case, the specimens had different levels of strain obtained during compression. The study [15] describes the effect of temperature, stress state and rolling direction on the fracture behavior of sheet material made of AZ31 alloy.

No test alone can provide an adequate description of the plasticity of a material. Therefore, the values of the limiting strain before failure are determined as a function of the stress triaxiality [16]. In this way, a diagram of ultimate plasticity is obtained. Sometimes the strain values are substituted for the shear ones. The stress triaxiality is varied by changing the type of test. Torsion of cylindrical specimens is used as one of the types of testing that provides a zero value of the average normal stress [17].

This study aims to determine the limiting strain before fracture of the magnesium alloy MA2-1 at a zero average normal stress. Additionally, the goal is to determine the inhomogeneities in the distribution of deformations in the applied method of specimen twisting.

MATERIAL AND TEST SETUP

Magnesium-based alloy MA2-1 additionally contains 0.3-0.7% manganese, 3.8-5.0% aluminum, 0.8-1.5% zinc. The area of applications of products from the MA2-1 alloy includes panels and stampings of complex configurations for welded structures. However, its maximum operating temperature is 150°C for long-term exposure and 200°C for short-term one. The advantages of using this alloy instead of aluminum alloys are the reduction in the weight of structures, as well as an increase in their degree of elasticity by reducing Young's modulus.

Determining the plastic properties of the MA2-1 magnesium alloy was carried out based on the results of torsion tests of a specimen with a cylindrical working part (Fig. 1a). The actual length of the working part $l = 30$ mm and the diameter $d = 7.45$ mm are due to the need to ensure the strength of the workpiece when machining a rolled bar with a diameter of $D = 12$ mm. To determine the strain distribution along the working part, a longitudinal gauge mark was mechanically applied to the lateral surface of the specimen (Fig. 1b).

Torsion tests were carried out on a test setup designed in the Ural Federal University. Figure 2 shows the main components of the equipment. The specimen is placed in the grips of test setup 1. If necessary, the specimen can be heated by passing an electric current through the sliding contact 2. The heating temperature is controlled using a pyrometer 6. The active grip of the test setup is rotated using a stepping motor 4 (SDS20-34100), connected to the rotating grip through a reduction planetary gearbox 3. The maximum value of the torque driven to the specimen is $T_{\max} = 100$ N·m. The control of the angle of rotation and angular velocity of the motor shaft is carried out using an encoder and controller built into the motor. The accuracy of the twist angle determination, taking into account the existing reducer, is $7.8 \cdot 10^{-5}$ radians. The sampling rate of the output signal from the controller is 100 Hz. To measure the actual value of the torque acting on the specimen, a TCN-10K sensor is provided, designed for a maximum torque $T_{\max} = 100$ N·m. The torque signal is characterized by a relative error of 0.05%. The registration of the signal is provided by an analog-to-digital converter ZET7111. The sampling frequency of the signal is 50 Hz.

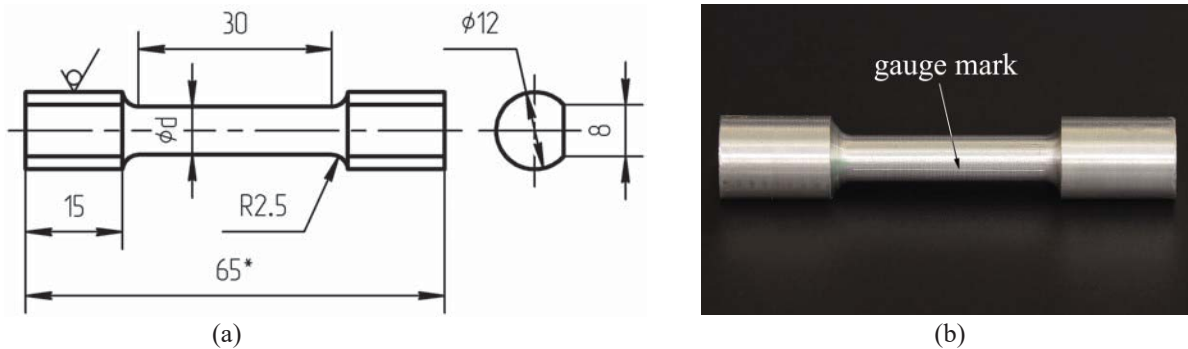


FIGURE 1. The geometry of the specimen (a) and the appearance of the gauge mark (b)



FIGURE 2. The torsion test setup: 1 – grips; 2 – sliding electric contact; 3 – planetary gearbox; 4 – step motor drive; 5 – torque sensor; 6 – pyrometer

METHOD FOR DETERMINING PLASTICITY

The specimen from the MA2-1 alloy was twisted at a rate of $\omega = 1$ rpm until fracture. In this case, the values of the torque T were recorded as a function of the specimen twist angle φ determined by the rotation angle of the active grip of the test setup. The values of shear strain in the specimen accumulated during the test were calculated by the formula [18]:

$$\Lambda = \frac{d}{2} \cdot \frac{\varphi}{l}. \quad (1)$$

According to Eq. 1, the strain values are considered to be distributed uniformly along the entire working part of the specimen. However, when testing cylindrical specimens, as a rule, the strain distribution is non-uniform. In this work, the inhomogeneity of the shear strain distribution along the working part of the specimen was estimated based on the inclination angle of the gauge mark to the generatrix γ . Due to the impossibility to fix the slope of the gauge mark during the test, the shear strain distribution was established only for the final stage of loading, i.e. at the moment of the failure of the specimen. Measuring the inclination angle was carried out by scanning the film wrapped on the specimen to transfer the gauge mark after unloading and subsequent processing of the obtained digital image. The measuring step along the axis of the specimen corresponded to a given scanner resolution of 600 dpi. Based on the obtained values of the angle of inclination of the gauge mark, the local values of the shear strain were calculated by the formula [18]:

$$\Lambda = \tan(\gamma). \quad (2)$$

It should be noted that the values of the shear strain calculated following Eq. 1 take into account not only the plastic but also the elastic component of strain since the values of the twist angle φ are determined directly during the test. At the same time, Eq. 2 allows only the residual plastic strain to be calculated.

RESULTS AND DISCUSSION

Figure 3 shows a diagram of the loading of the specimen. Typical sections of the diagram are the elastic loading stage 1, plastic deformation stage 2 with the material hardening, and stage 3 corresponding to the specimen softening. Note that, in the general case, the softening of the specimen can be associated with:

- changes in the grain structure of the material in a hot state, for example, polygonization, recrystallization, etc.;
- changing the material flow mechanism;
- a decrease in the bearing capacity of the specimen determined by the cross-sectional area;
- the formation and development of defects.

In our case, the test was carried out in a cold state, and the cross-sectional area of the specimen, as a rule, does not change or changes insignificantly during torsion. Therefore, the softening of the specimen can be associated with structural changes or the formation of defects. Examination of the specimen after fracture revealed a longitudinal crack located at some distance from the gauge mark (Fig. 4a). Figure 4b makes it possible to evaluate the size of this crack extending into the depth of the specimen.

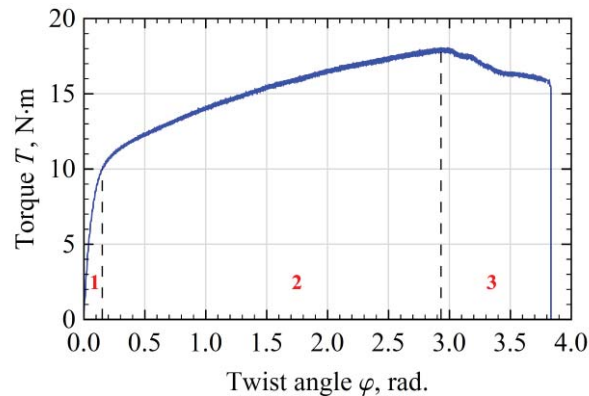


FIGURE 3. The loading diagram: 1 – the stage of elastic deformation; 2 – the stage of plastic deformation with the hardening; 3 – the softening stage

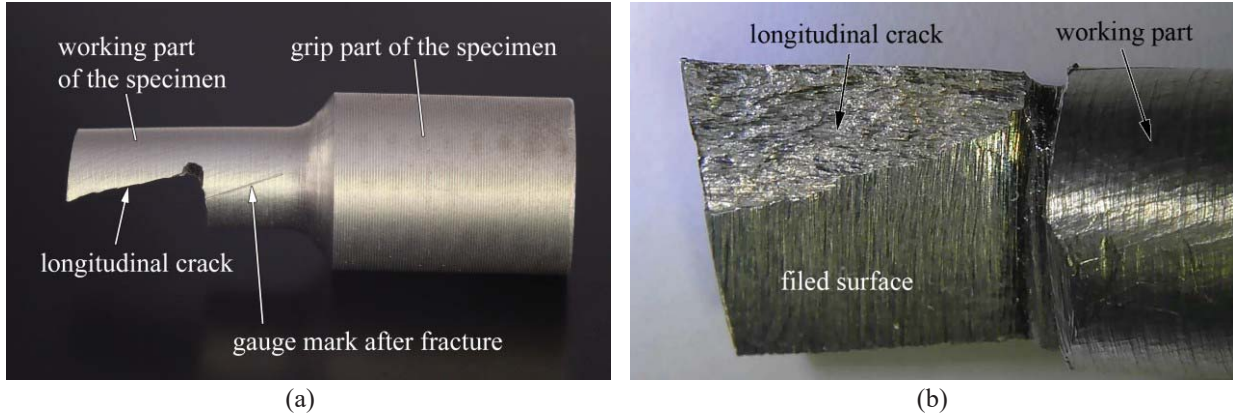


FIGURE 4. The right part of the specimen after fracture: (a) – the location of longitudinal crack; (b) – the close-up photography of the longitudinal crack

The longitudinal crack (Fig. 4) was formed on both halves of the specimen before fracture. To estimate the depth of the crack the right part of the specimen was filed. The filing was carried out at an angle to the plane of the longitudinal crack. It was made a cut using a metal hacksaw to separate the part of the specimen that includes one of the surfaces of the crack. It took a little force to remove this part. As a result, it was possible to establish a clear boundary of the crack. As seen from Fig. 4b, the crack depth is maximal in the plane of transverse fracture of the specimen.

Figure 5a shows the involute of the applied mark after the fracture of the specimen. Here, the z coordinate corresponds to the direction of the specimen axis, and the y coordinate is the arc length along which the points on the gauge mark moved during testing the specimen, fracture, and elastic unloading. Figure 5b shows the distribution of the shear strain, calculated according to Eq. 2, along the specimen axis.

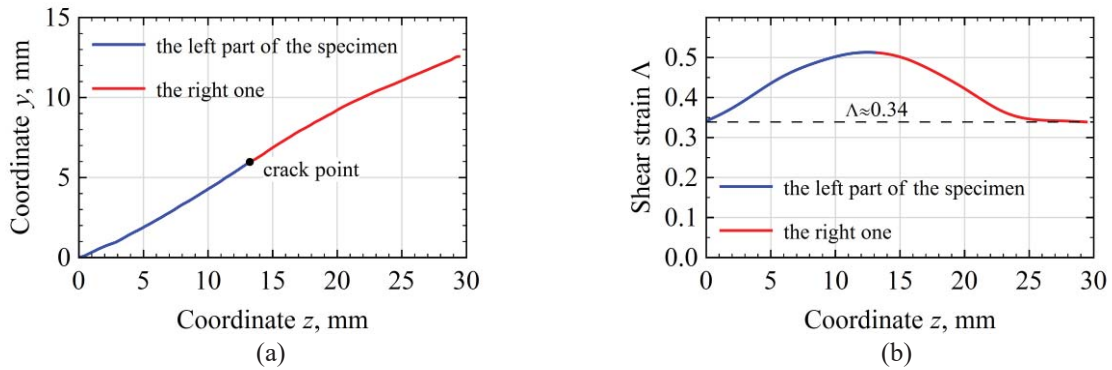


FIGURE 5. The involute of the gauge mark after specimen fracture (a) and the shear strain calculated based on it (b)

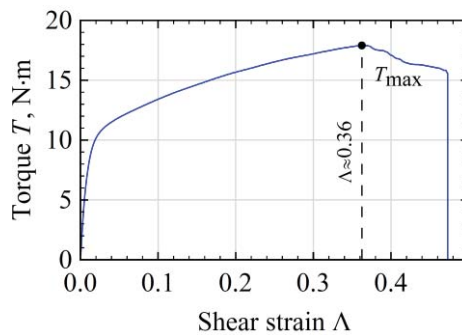


FIGURE 6. The loading diagram based on shear strain values

One can see that the shear strain values on the left and right parts of the specimen far from the fracture section are the same and are approximately $\Lambda = 0.34$. In addition, as seen from Fig. 4, the crack is of limited length. Thus, the indicated value of the shear strain corresponds to a continuous section of the specimen without a defect, i.e. to the moment preceding the initiation of the crack. Figure 6 also confirms this conclusion. It shows torque versus shear strain calculated by Eq. 1. It can be seen that at the shear strain equal to $\Lambda = 0.36$ the stage of specimen softening begins, i.e. the crack starts to form. Taking into account elastic unloading, this value is equal to the shear strain in the areas adjacent to the grips (Fig. 5b).

Taking into account the obtained data on the distribution of shear strain along the specimen, as well as the loading diagram, it can be concluded that the actual value of the ultimate plasticity of the magnesium alloy MA2-1 is $\Lambda_{ult} = 0.34 \dots 0.36$.

CONCLUSION

The obtained data on the deformation distribution along the specimen as well as loading diagram indicate a low level of plasticity of MA2-1 alloy at a zero average normal stress. Established value of the ultimate plasticity is equal to $\Lambda_{ult} = 0.34 \dots 0.36$. Therefore, it is advisable to carry out cold deformation under artificially created additional pressure, for example, with the use of some extrusion scheme, as well as the use of shells [7, 8, 20].

ACKNOWLEDGMENTS

The reported study was funded by RFBR, project number 20-38-90051. The study was performed within the framework of the state assignment (theme "Pressure" No. AAAA-A18-118020190104-3).

REFERENCES

1. W.J. Joost and P.E. Krajewski, *Scripta Materialia* **128**, 107-112 (2017).
2. A. Chapuis and J.H. Driver, *Acta Materialia* **59**, 1986-1994 (2011).
3. F. Liu, C. Chen, J. Niu, J. Pei, H. Zhang, H. Huang, and G. Yuan, *Materials Science and Engineering C* **48**, 400-407 (2015).
4. B. Song, R. Xin, Y. Liang, G. Chen, and Q. Liu, *Materials Science and Engineering A* **614**, 106-115 (2014).
5. M.R. Barnett, Z. Keshavarz, A.G. Beer, and D. Atwell, *Acta Materialia* **52**, 5093-5103 (2004).
6. D.R. Nugmanov, O.Sh. Sitdikov, and M.V. Markushev, *The Physics of Metals and Metallography* **116**, 993-1001 (2015).
7. D.A. Komkova, O.V. Antonova, and A.Y. Volkov, *Physics of Metals and Metallography* **119(11)**, 1120-1126 (2018).
8. B.I. Kamenetskii, Y.N. Loginov, and N.A. Kruglikov, *Russian Journal of Non-Ferrous Metals* **58(2)**, 124-129 (2017).
9. A. R. Ragab, *Materials Science and Engineering: A* **334(1-2)**, 114-119 (2002).
10. J. L. Dequiedt and C. Denoual, *International Journal of Solids and Structures* **210-211**, 183-202 (2021).
11. K. Yoshida, *International Journal of Plasticity* **84**, 102-137 (2016).
12. B. Behrens, A. Chugreev, and M. Dykiert, *Procedia Manufacturing* **29**, 450-457 (2019).
13. Y. Jia and Y. Bai, *International Journal of Fracture* **197**, 25-48 (2016).
14. B. Song, R. Xin, Y. Liang, G. Chen, and Q. Liu, *Materials Science and Engineering A* **614**, 106-115 (2014).
15. Y. Jia and Y. Bai, *International Journal of Fracture* **197**, 25-48 (2016).
16. M. Ganjiani and M. Homayounfar, *International Journal of Solids and Structures* **225**, 111066 (2021).
17. M. V. Erpalov and D. A. Pavlov, *IOP Conference Series: Materials Science and Engineering* **971(4)**, 042025 (2020).
18. V.L. Kolmogorov, *Studies in Applied Mechanics* **43**, 219-233 (1995).
19. V.L. Kolmogorov, *Journal of Materials Processing Technology* **70**, 190-193 (1997).
20. Yu.N. Loginov and Yu.V. Zamaraeva, *Metal Working and Material Science* **23(1)**, 79-88 (2021).